CO-6-9106289--6

MAY 28 1992

LBL-31886
UC-414

Lawrence Berkeley Laboratory
UNIVERSITY OF CALIFORNIA

Physics Division

Presented at the Third Topical Seminar on Heavy Flavors, San Miniato, Tuscany, Italy, June 17-21, 1991 and to be published in the Proceedings

Heavy Flavor Physics at Hadron Colliders

A. Barbaro-Galtieri

December 1991

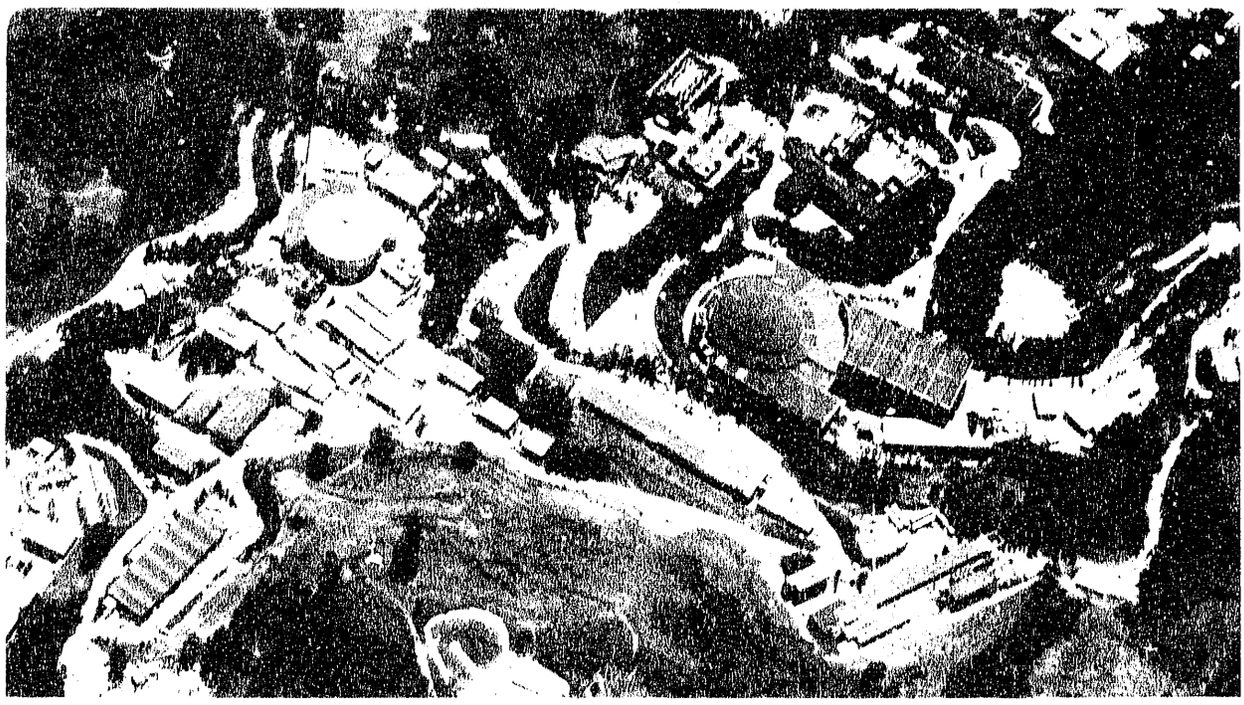

Prepared for the U.S. Department of Energy under Contract Number DE-AC03-76SF00098

DISTRIBUTION OF THIS DOCUMENT IS UNLIMITED

DISCLAIMER

This document was prepared as an account of work sponsored by the United States Government. Neither the United States Government nor any agency thereof, nor The Regents of the University of California, nor any of their employees, makes any warranty, express or implied, or assumes any legal liability or responsibility for the accuracy, completeness, or usefulness of any information, apparatus, product, or process disclosed, or represents that its use would not infringe privately owned rights. Reference herein to any specific commercial product, process, or service by its trade name, trademark, manufacturer, or otherwise, does not necessarily constitute or imply its endorsement, recommendation, or favoring by the United States Government or any agency thereof, or The Regents of the University of California. The views and opinions of authors expressed herein do not necessarily state or reflect those of the United States Government or any agency thereof or The Regents of the University of California and shall not be used for advertising or product endorsement purposes.

Lawrence Berkeley Laboratory is an equal opportunity employer.

LBL--31886

DE92 014482

Heavy Flavor Physics at Hadron Colliders[1]

Angela Barbaro-Galtieri

Lawrence Berkeley Laboratory
University of California
Berkeley, CA 94720

December 1991

[1]This work was supported by the Director, Office of Energy Research, Office of High Energy and Nuclear Physics, Division of High Energy Physics of the U.S. Department of Energy under Contract DE-AC03-76SF00098.

MASTER

DISTRIBUTION OF THIS DOCUMENT IS UNLIMITED

HEAVY FLAVOR PHYSICS AT HADRON COLLIDERS

Angela Barbaro-Galtieri
Lawrence Berkeley Laboratory, University of California, 1 Cyclotron Road, Berkeley, CA 94720*

The search for the top quark has dominated heavy flavor physics at hadron colliders. For Standard model decay of top the present mass limit is $m_t > 89$ GeV(95% C.L.) . Bottom production cross sections are quite large at hadron colliders, thus providing enough statistics for extensive studies. Results on cross sections, $B^0 - \overline{B}^0$mixing, exclusive channels and rare B decays will be summarized.

1 INTRODUCTION

The Standard Model includes three lepton and three quark doublets. Apart from a lack of direct observation of the ν_τ, the top quark is the last missing block of the model. The measurement of backward-forward asymmetry in $e^+e^- \to b\bar{b}$ and the absence of flavor changing neutral currents in b decays provide indirect evidence for the existence of an isodoublet partner of the bottom quark. The CDF experiment at the Tevatron Collider has reported a lower mass limits (95% C.L.) of 89 GeV[1]. Recent fits to the Standard Model parameters, including radiative corrections to the W and Z masses, provide an upper limit of $m_t < 210$ GeV[2]. We will review these results and discuss prospects for the future.

The cross section for b pair production at hadron colliders is predicted from QCD to be quite large (about 50 μb at the Tevatron Collider). The b cross section measurements of UA1 and CDF and their comparison to theoretical calculations will be discussed. Also, $B^0 - \overline{B}^0$mixing measurements of UA1 and CDF will be reviewed. Because of the copious b production exclusive channels are now being detected by CDF, and limits on rare decay modes are reported by both CDF and UA1.

2 TOP SEARCH

Top production at a hadron collider can take place through the electroweak process $p\bar{p} \to W \to t\bar{b}$ or the hard scattering process $p\bar{p} \to t\bar{t}$. For the first process to occur the top mass has to be below the W mass. Figure 1 shows the total cross sections for the two processes[3] at $\sqrt{s} = 0.63$ and 1.8 TeV. At CERN energies the electroweak process dominates, whereas at the Tevatron Collider the top production rate from hard scattering dominates. The hard scattering cross sections of Figure 1 are obtained by combining the higher order calculations of Nason et al[4] with the structure functions of Diemoz et al.[5], using the method of Altarelli et al.[6].

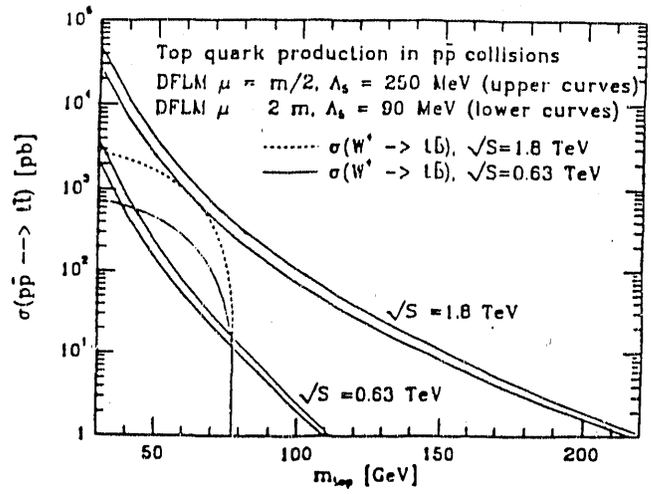

Figure 1: Top pair production cross section versus top mass[3-6]. The bands represent the uncertainty due to Q^2 scale and range in Λ_{QCD} (5 flavors). The $W \to t\bar{b}$ cross section is also included. Both Tevatron and CERN energies are shown.

2.1 STANDARD TOP DECAYS

The $t \to Wb$ decay of the top quark via the charged weak current into a bottom quark and a virtual W (real for

*This work was supported in part by the Director, Office of Energy Research, Office of High Energy and Nuclear Physics, Division of High Energy Physics of the U.S. Department of Energy under Contract DE-AC0376SF00098.

$m_{top} > m_W + m_b$), provides the signatures to be exploited for a top search. The most copious channel is provided by the hadronic decay modes, which, however, suffers from severe backgrounds from QCD. A much cleaner signature is provided by the leptonic decay of the W, as these leptons have high P_T and are isolated. Analyses have been done on a. events with one high P_T lepton and jets, b. events with two high P_T leptons, one from each W, and c. events of category a. with the requirement of an additional low P_T lepton coming from the semileptonic decay of the b quark (b tag).

Backgrounds to semileptonic decays of top come from other physics processes and from lepton misidentification. The Drell-Yan process, W, Z production and $b\bar{b}$ pair production are sources of high P_T leptons. These processes have to be understood in order to assess their contribution to the signals. For the lepton+jets final state the major background is due to $b\bar{b}$ and W+jets production. For the dilepton channels it is due to $b\bar{b}$, Drell-Yan, and $Z^0 \rightarrow \tau\bar{\tau}$ production. For the ee and $\mu\mu$ final states the Z mass region has to be removed altogether.

The results of the measurement made and the channel used are summarized in Table I. The most recent measurements are from CDF, where results from the $e\mu$, ee, $\mu\mu$, and ℓ + jets with a b tag ($b \rightarrow \mu$) channels have been combined. After selection of events, proper cuts to reduce non lepton background and kinematic cuts to reduce the physics background, only one candidate event is left in the 4.1 pb^{-1} analyzed in the $e\mu$ channel. Figure 2 shows the electron transverse energy (E_T) plotted versus the muon transverse momentum (P_T). The signal region is above 15 GeV for both variables. The one candidate at high E_T and high P_T is consistent with background calculations: 0.2 events from $Z^0 \rightarrow \tau\bar{\tau}$ and 0.2 events from $Z^0 \rightarrow b\bar{b}$. The expected number of events for WW production is 0.15 and for WZ is 0.05. For leptons of such high momenta ($E_T^e >$ 30 GeV and $P_T^\mu >$ 40 GeV/c) the probability of $Z^0 \rightarrow \tau\bar{\tau}$ is $\leq$ 1%.

From these data, when the systematic uncertainties on luminosity, acceptance, detection efficiency etc., are convoluted with the Poisson distribution for the one event, the

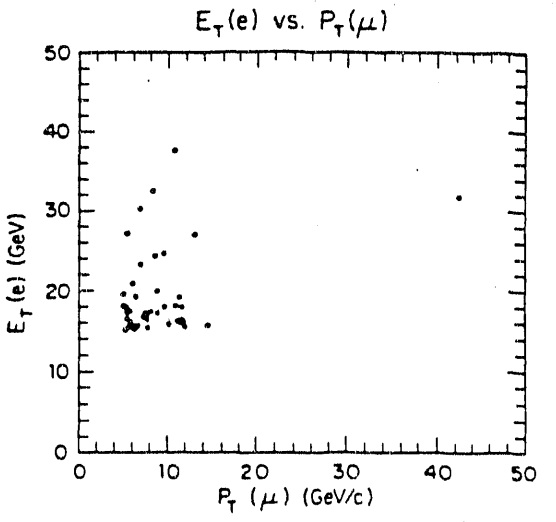

Figure 2: Electron transverse energy versus muon transverse momentum for the CDF $e\mu$ events[10].

Table 1: Top quark mass limits from UA1,UA2,CDF

Experiment	Channel	Limit(95% C.L.) (GeV)
UA1[7]	ℓ+ jets,$\mu\mu$	$m_t > 60$
UA2[8]	e+ jets	$m_t > 69$
CDF[9]	e+ $\geq$2 jets	$m_t > 77$
CDF[10]	$e\mu$	$m_t > 72$
CDF[1]	combines $e\mu$, ee, $\mu\mu$, $b \rightarrow \mu$	$m_t > 89$

cross section upper limits of Figure 3 are obtained. The lowest value of the theoretical cross section intersects the experimental limit at 89 GeV. Assuming that top decays exclusively via the charged current mode ($t \rightarrow Wb$) the preliminary CDF result[1] thus is:

$$m_t > 89\ GeV \quad \text{with 95\% C.L.}$$

2.2 NON STANDARD TOP DECAYS

The top mass could be lower than 89 GeV if the predominant decays are other then those predicted by the Standard Model. For example, were a charged Higgs(H^+) of mass smaller than that of the W to exist, the top could decay as $t \rightarrow H^+b$ with a large branching ratio. For a top mass in the range $m_{H^+} + m_b < m_t < m_W + m_b$ the decay into H^+b would be about 100%. The decay modes

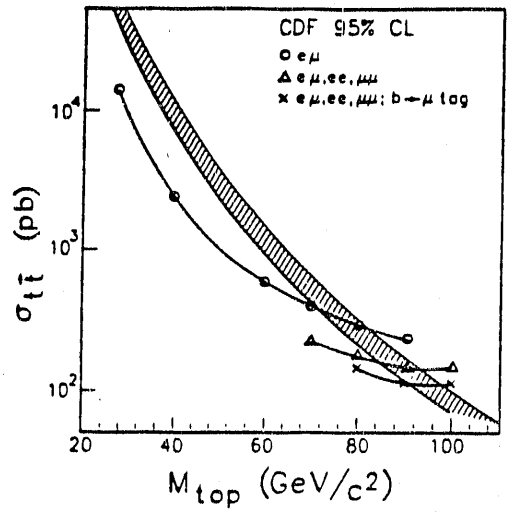

Figure 3: The 95% C.L. upper limit of the top cross section as a function of the top mass, for several sets of CDF data: the published $e\mu$ data[10], the combination of all di-lepton channels, and the combination of the di-lepton channels and the lepton+2jets+low energy μ channels[1].

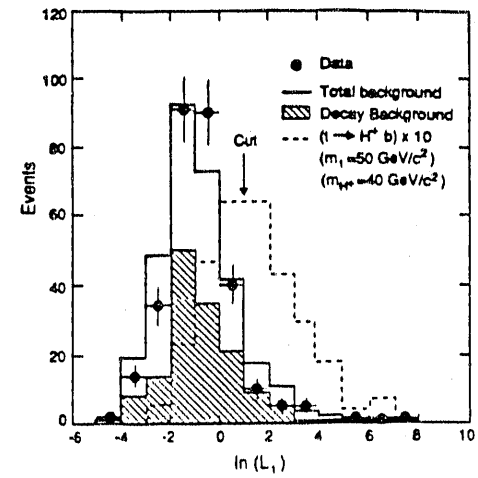

Figure 4: The distribution of $\ln(L_1)$ for single μ events as obtained by the UA1 collaboration[12]. The data is compared to the Monte Carlo simulation of all the known background processes and the $t \rightarrow H^+b$ hypothesis, for m_t = 50 GeV, m_{H^+} = 40 GeV and $BR(H^+ \rightarrow \tau\nu) = 95\%$.

of the H^+ depend on the Higgs model used[11]. In the simple extension of the Standard Model, there are two Higgs doublets which result in both charged and neutral Higgs bosons. The H^+ branching ratios depend on the couplings of the two Higgs doublets to quarks and leptons. The couplings depend on a parameter, $\tan\beta$, which is the ratio of the vacuum expectation values of the neutral components of the two Higgs doublets. For large values of $\tan\beta$ the dominant H^+ decay is $\tau\nu$, for small values of $\tan\beta$ the dominant decay is H^+ into $c\bar{s}$. The searches reported above would not detect such decay modes.

The UA1 experiment[12] has searched for an excess of τ over μ and e from W's. The process is $t \rightarrow H^+b$ with subsequent decay of $H^+ \rightarrow \tau\nu$. The topologies studied are $\mu+ \geq 2$ jets and $\mu\mu+$ jet, for the case where the b itself decays into a μ (non-isolated). This study is done by maximum likelihood method involving more then one variable. For the single muon analysis the variables used are: P_T of the muon, E_T^{miss} and $|cos\theta_{j2}|$, where θ_{j2} is the angle of the second highest E_T jet and the beam axis in the rest frame of the system μ-jet$_1$-jet$_2$-E_T^{miss}. The distribution of the likelihood of the different hypotheses is shown in Figure 4. The H^+ hypothesis clearly does not fit the data, which is well explained by background. For this plot $\tan\beta$=2 is assumed, this gives $BR(H^+ \rightarrow \tau\nu) \geq 93\%$.

The top mass limit depends on the value of the H^+ mass and of the parameter $\tan\beta$ that determines the $H^+ \rightarrow \tau\nu$ branching ratio. The final result, for a 95 % branching ratio is shown in Figure 5. This puts a limit to the top mass $m_t > 60$ GeV for m_{H^+} =43 GeV.

2.1 TOP MASS FROM EWK PARAMETERS

The measurement of the W mass at hadron colliders also provides information on the top mass, since it is related to the vector boson masses through the radiative corrections, Δr. In the standard electro-weak gauge theory, Δr can be calculated perturbatively as the sum of many terms:

$$\Delta r = \Delta r^{(\alpha)} + \Delta r^{(\alpha*\alpha_S)} + \Delta r^{(\alpha^2)} + ... \qquad (1)$$

In Δr there are contributions proportional to m_t^2 resulting from virtual top quark effects which affect the W and Z propagator. The appearance of these terms is a direct consequence of the Higgs origin of the top quark mass. The top mass has a less strong dependence on the Higgs mass itself.

The W mass has been recently measured at hadron colliders with high precision by UA2[15] and CDF[16]. The results are:

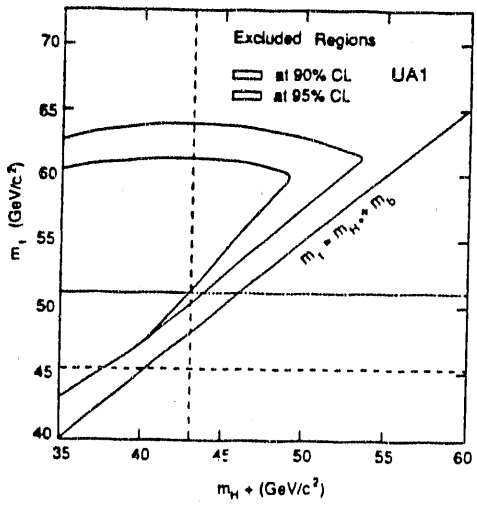

Figure 5: The 90% and 95% C.L. upper limit on the top mass as a function of the H^+mass as obtained by the UA1 experiment[12] assuming $BR(H^+ \rightarrow \tau\nu) = 95\%$. The dashed lines delineate regions excluded at the 95% C.L. by e^+e^- experiments[13], the dotted line shows the limit obtained at 90% C.L. by measurement of the W total width, Γ_W, by CDF[14].

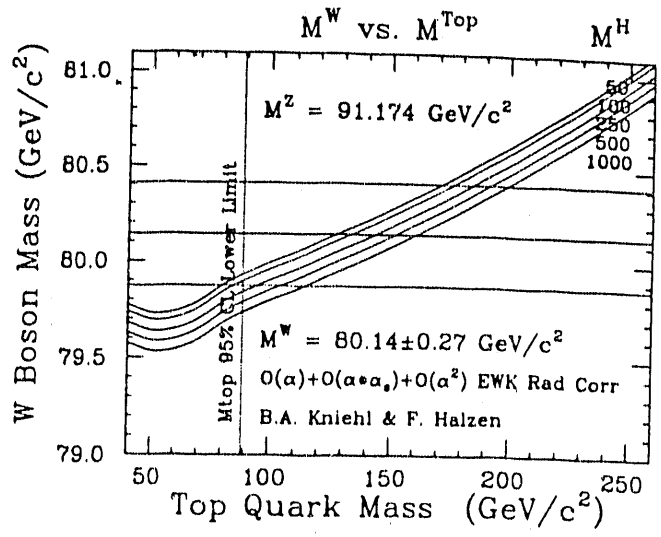

Figure 6: Dependence of the W mass on the top mass as calculated from radiative corrections to the vector boson masses by Halzen and Kniehl[17]. The average of the W mass measurements obtained by UA2[15] and CDF[16] is shown as a band for a one standard deviation error.

$M_W = 80.35 \pm 0.37$(stat. and syst.) GeV UA2

$M_W = 79.91 \pm .39$ (stat. and syst.) GeV CDF

with average:

$M_W = 80.14 \pm .27$ GeV

The radiative corrections have been recently calculated with the higher order loop contributions by Halzen and Kniehl[17]. Their prediction is shown in Figure 6. The average W mass above is plotted as a band; the Z mass value of 91.174 is an average of the LEP results[18]. The top mass limits are as follows:

$m_t = 142^{+46}_{-41}$ GeV for $M_H = 250$ GeV

and the central value dependence on the Higgs mass is:

$m_t = 142^{+15}_{-18}$ GeV for $M_H = 50$-1000 GeV

the combination of the two uncertainties (see Figure 6) gives the limit $m_t < 200$ GeV (90% C.L.). For fits of these data as well as the LEP and ν scattering data, see the analyses reported in Ref. 2.

3.0 B PHYSICS AT HADRON COLLIDERS

Cross sections for b quark production are quite large at hadron colliders. In recent years, both UA1 and CDF have been studying mixing, exclusive and rare decays. We will survey here those results. Details of some of the CDF results can be found in the contribution by Hans Wenzel in these Proceedings[19].

3.1 BOTTOM CROSS SECTION

Nason, Dawson and Ellis (NDE)[4], have calculated bottom production cross sections at hadron colliders to next to leading order (NLO) QCD.

Large uncertainty in the cross sections arise from uncertainties in the choice of the scale (μ), Λ_{QCD}, the bottom mass, and the the choice of structure functions. Figure 7 shows the results of ref. 4,3 for a range of values for these quantities.

Cross section measurements have been done by the UA1 and CDF collaborations. One of the methods used by both experiments has been the study of the inclusive lepton spectrum, which exploits the copious semileptonic decays of the B hadrons. Backgrounds to this final state come from leptons from charm decays, from W and Z production, and from hadrons misidentified as leptons. The major systematic errors come from uncertainties in the bottom quark fragmentation, the semileptonic branching ratio and the assumed bottom P_T distribution for accep-

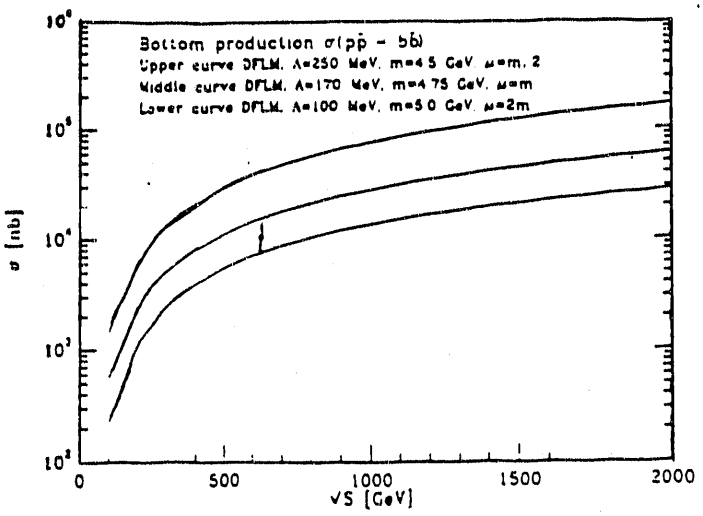

Figure 7: Bottom cross section as a function of $\sqrt{s}$ as calculated by Nason et al[4,3]. Uncertainties due to Λ_{QCD}, choice of scale, and bottom mass are also shown. The structure functions used are from Diemoz et al[5].

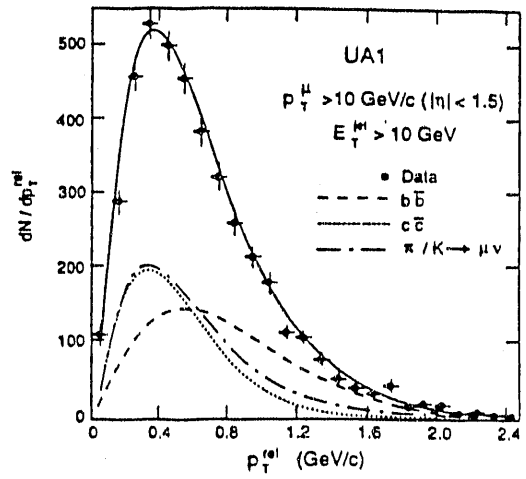

Figure 8: The UA1 distribution of muon P_T relative to the b jet axis[20]. The $b\bar{b}$ and $c\bar{c}$ curves shown are calculated with the ISAJET[21] Monte Carlo, whereas the background is estimated from π/K decays.

tance calculation.

3.1.1 THE UA1 MEASUREMENTS

The UA1 analysis[20] is based on a sample of 6103 muons with $P_T > 10$ GeV/c in an $|\eta| < 1.5$ interval. At least one jet is required with $P_T > 10$ GeV/c and separation from the muon of more than $\Delta R = 1.0$. Here $\Delta R = \sqrt{\Delta(\phi)^2 + \Delta(\eta)^2}$, where ϕ is the azimuthal angle and η the pseudorapidity. The direction of the jet to which the μ belongs is obtained by using only the charge particles (including the muon) within a cone of $\Delta R < 0.6$ with the μ direction. The variable used to study this sample is the P_T of the μ relative to the jet axis.

After additional requirements (including non-isolation) for removal of W and Z production, UA1 obtains[20] the distribution of P_T^{rel} shown in Figure 8. The contribution from bottom, charm, and hadron backgrounds, as obtained from Monte Carlo, are shown. The result of the fit gives the fraction of $b\bar{b}$ events to be 0.33 ± 0.03(stat) ± 0.03 (syst).

These data provide b cross section measurements for μ P_T above 10 GeV/c. The data is divided in bins to provide an inclusive integrated cross section for P_T^b greater then that of the assigned bin (determined by requiring that 90% of the muons come from b quarks with momentum above that bin value). The lowest P_T^b bin from inclusive muons is at 15 GeV/c. The systematic uncertainties come from b quark fragmentation (± 6%), integrated luminosity (± 8%), detector acceptance (± 8%), $b \rightarrow \mu$ branching ratio (assumed to be (10.2 ± 1.0)%), jet E_t scale (± 12%), and the assumed b quark spectrum (± 20%).

The results are shown in Figure 9 superimposed to the NDE calculations[4]. In Figure 9 results from di-muon events are also shown: for $P_T > 6$ GeV/c (J/ψ events), $P_T > 6$ GeV/c (low mass di-muon events), and $P_T > 10$ GeV/c (high mass di-muon events). These analyses are described in Ref. 20,22. The agreement between the measurements and the calculations is quite good, within the experimental and theoretical uncertainties, for a P_T^{min} range from 6 to 54 GeV/c.

Normalizing the QCD predictions of Figure 9 to the first three data points and extrapolating to $P_T^{min} = 0$, they obtain a prediction for the inclusive b cross section of 12.8 ± 4.7(exp.) ± 6(th.) μb in the rapidity range $|\eta| < 1.5$. Using the QCD rapidity distribution they obtain σ ($p\bar{p} \rightarrow b\bar{b}$+X) = 19.3 ± 7(exp) ± 9(th.) μb at $\sqrt{s} = 630$ GeV.

3.1.2 THE CDF MEASUREMENTS

The CDF collaboration has measured the b quark cross section at $\sqrt{s} = 1.8$ TeV using the inclusive electron spec-

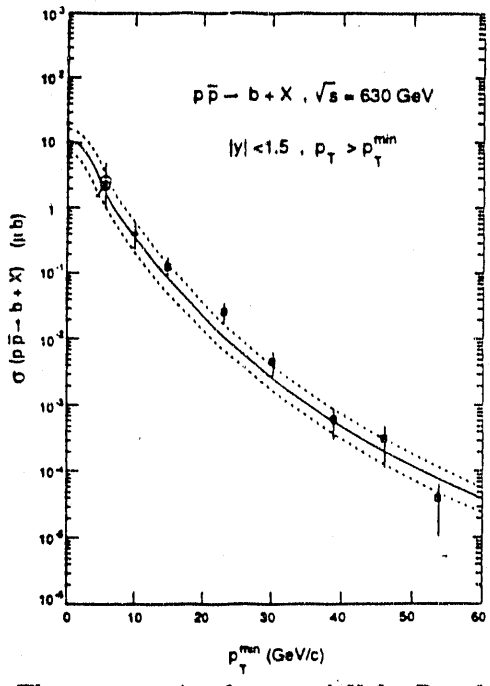

Figure 9: The cross section for $p\bar{p} \to b$ X for P_T of b quark above P_T^{min} plotted versus P_T^{min}, as obtained by UA1[20,22] (data points), compared to the calculations of Nason et al[4] (curves).

trum and the $\psi K^{\pm}$ exclusive channel. The P_T range covered is 10-32 GeV/c.

The electron sample was obtained with two separate triggers. The 12 GeV electron trigger required a central calorimeter electromagnetic (EM) shower with cluster $E_T > 12$ GeV, accompanied by a charged track with $P_T >$ 6 GeV/c pointing to it. The 7 GeV trigger had similar requirements but was prescaled. A total of 4.4 pb^{-1} and 175 nb^{-1} were collected for the two triggers, respectively. Electron identification in CDF relies on the fine calorimeter segmentation and the use of proportional chambers located at shower maximum in the calorimeter[16,23]. In order to reduce the hadron background (π^0 overlapping with charged tracks) for electron energies as low as 7 GeV, more stringent requirements are applied to this sample[24].

Photon conversion electrons and Dalitz pairs (from $\pi^0 \to e^+e^-\gamma$) are removed by rejecting events that have a second charged track, of opposite sign, that forms a low invariant mass pair with the electron. This algorithm, however, removes only 50% of the photon conversions, leaving a contamination estimated to be (20 ± 5)% of the electron

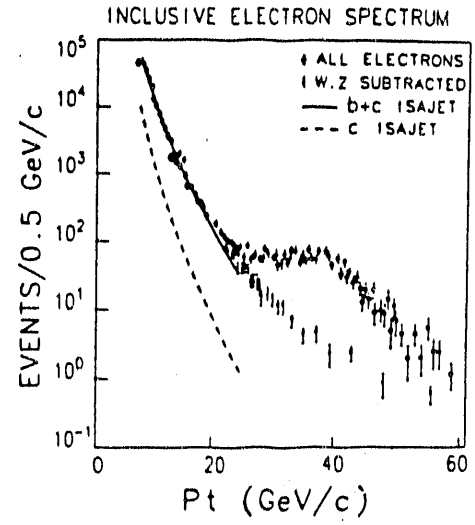

Figure 10: The CDF inclusive electron spectrum[24] for both the 7 and the 12 GeV electron triggers, as function of electron P_T. The lower set of points represents the spectrum after the W and Z contributions have been removed. The dashed line represents the charm contribution as calculated using the ISAJET Monte Carlo[21].

sample. The electron spectrum thus obtained is shown in Figure 10.

The contribution of the electrons from W is removed by requiring that the event have a $E_T^{miss} < 8\sqrt{E_T}$, where E_T is the total transverse energy in the event, obtained adding all the calorimeter cells. The contribution from Z decays is removed by rejecting events for which there is a second electron that gives a di-electron invariant mass greater than 80 GeV.

Remaining backgrounds are from hadrons misidentified as electrons and electrons from charm. The first contamination is estimated to be (15 ± 15)% from a study of the electron selection variables. The charm contribution is estimated to be (12 ± 10)% from the ISAJET Monte Carlo[21]. Supporting evidence that this sample contains mostly electrons from the b quark is shown in Figure 11. Here a search is made for the decay $\overline{B} \to e^- D^0 X$, where the D^0 decays into a $K^-\pi^+$, i.e., the e and the K have the same sign. The correct (wrong) sign combinations, for $\overline{B} \to e^- D^0 X$ and its charge conjugate decay, are shown in Figure 11a (11b). There are 75 ± 17 events with the correct sign combination in agreement with the calculated rate obtained using the measured branching ratios for this

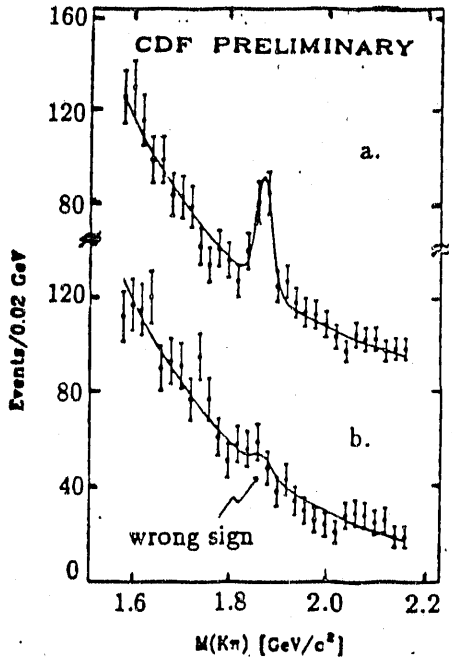

Figure 11: The $K^{\pm}\pi^{\mp}$ invariant mass spectrum for tracks within a cone of $\Delta R = 0.6$ around the high P_T electron. a. Combinations for which the e and the K have the correct sign to be decay products of a B meson. b. Wrong sign combinations.

decay mode.

To relate the electron spectrum to a parent b quark, CDF used the same technique as employed by UA1 and previously described. The cross sections are calculated for three P_T bins. The systematic errors from sources other than backgrounds come from the uncertainties in b quark fragmentation (16%), electron identification efficiency (10%), trigger efficiency (10%), B semileptonic branching ratio (10%) and integrated luminosity (7%). The results are shown in Figure 12, where the cross sections calculated by Nason et al[4] are also shown for comparison.

The second method used by CDF[24] to measure the b cross section consists in reconstructing $B^{\pm}$ mesons decaying into $\psi + K^{\pm}$. The ψ sample was obtained by triggering on two muons using the central muon chambers ($|\eta| < 0.65$). Two triggers were used, which required two muons with $P_T > 3$ GeV/c, or $P_T > 5$ GeV/c. These were implemented at different times during the run. The integrated luminosities were of 2.63 pb^{-1} and 1.61 pb^{-1} respectively.

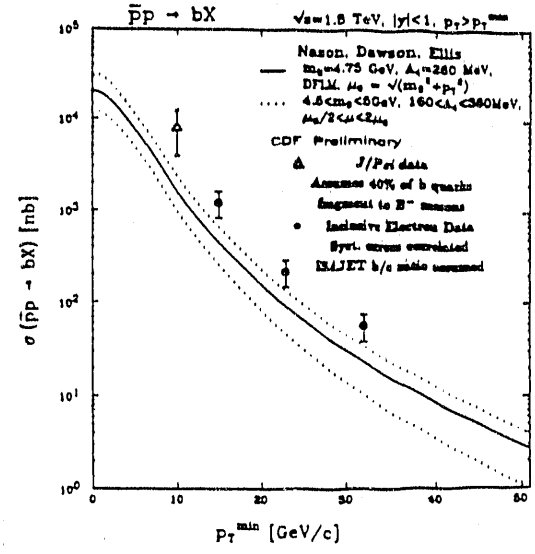

Figure 12: The b quark inclusive production cross section for P_T of the b quark above P_T^{min} versus P_T^{min}, as measured by CDF[24]. Here $|\eta| < 1.0$ was required for the b quark. The lowest P_T point comes from the channel $B \rightarrow \psi K^{+}$, the other three points come from the inclusive e spectrum.

The invariant mass distributions for same and opposite sign muons are shown in Figure 13. The ψ signal is clearly visible in the opposite sign di-muon mass spectrum. The standard CDF muon selection criteria have been applied to this sample[16]. The J/ψ sample is obtained by requiring the invariant mass of the two muons to be 3097 ± 50 MeV and consists of 2500 events. The average P_T for the J/ψ is 8 GeV/c, due to the trigger requirements.

To reconstruct a given final state, the two muons from the J/ψ are first constrained to the beam position and then mass constrained to improve the resolution. Next all tracks found in a cone of 60^0 around the J/ψ direction are combined with the J/ψ, using the relevant mass assignment for the required final state. For the decay $B^{\pm} \rightarrow J/\psi + K^{\pm}$ the track is required to have a $P_T > 3$ GeV/c. For the $J/\psi + K^{*0}$ final state only the three highest tracks are used to form the $K\pi$ combinations, in order to reduce the combinatorial background. The invariant mass distribution for these two final states is shown in Figure 14. The signal at the B mass includes 35 ± 9 events[24].

To measure the b quark cross section only the $P_T > 3$ GeV/c trigger sample was used, containing (10.5 ± 4.0) $B^{\pm} \rightarrow J/\psi + K^{\pm}$ events. The branching ratio for B deca,

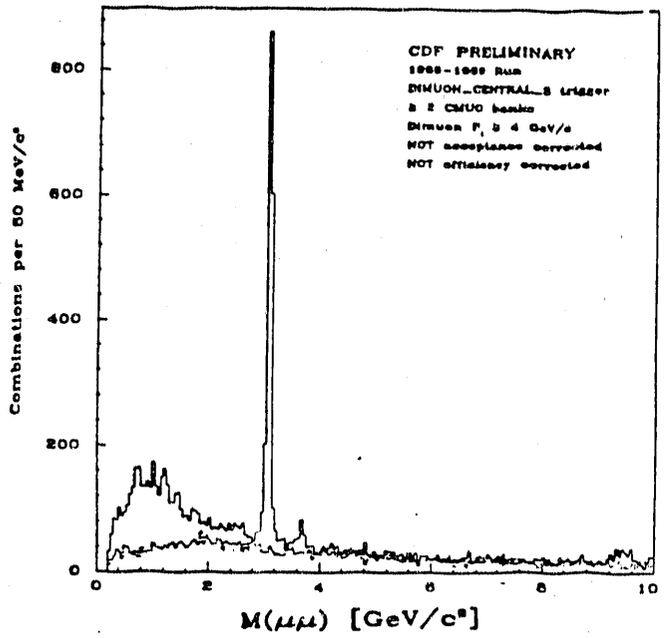

Figure 13: The invariant mass distribution of the two muons in di-muon trigger events in CDF[24]. The lower histogram represents the same charge combinations, the upper one the opposite charge combinations.

in this final state with subsequent $J/\psi \rightarrow \mu^+\mu^-$ has been measured by both CLEO[25] and ARGUS[26]. The average is:

$$Br(B^\pm \rightarrow J/\psi + K^\pm,\ J/\psi \rightarrow \mu^+\mu^-) = (5.2 \pm 1.2) \times 10^{-5}$$

In order to calculate the acceptance and the b quark spectrum corresponding to the reconstructed B mesons, a simple Monte Carlo was used. The b quark spectrum was generated according to the NDE calculations[4], flat in rapidity for $|\eta| < 1.0$, the b quark was then fragmented according to the Peterson fragmentation function[27]. Finally, the $B^\pm$ was assumed to be produced 40% of the times. Applying the analysis requirements CDF finds that 90% of the reconstructed B's come from b quarks with $P_T > 10$ GeV/c.

The uncertainty on the branching ratio constitutes the major systematic error in the cross section determination. Other contributions come from uncertainties on b quark fragmentation (10%), tracking efficiency (10%), trigger efficiency (12%), and other smaller contributions. The result is shown in Figure 12. All the CDF cross section measurements appear to be larger then the expectation from the NDE calculation. At $\sqrt{s} = 630$ GeV instead, the agreement seems to be very good (Figure 9).

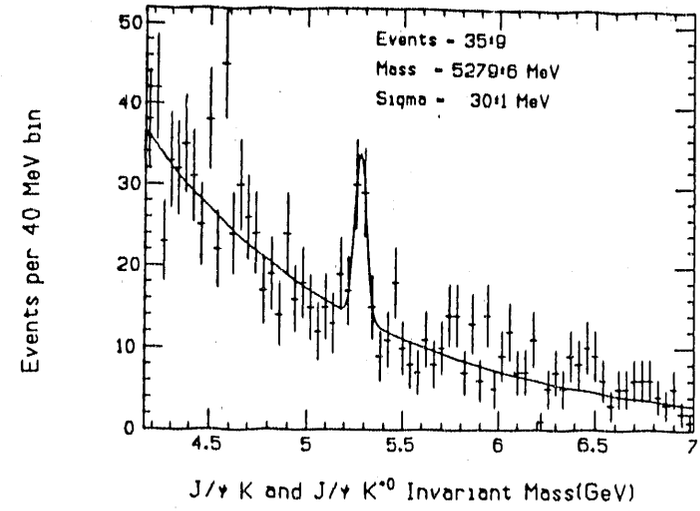

Figure 14: The combined invariant mass spectrum for the channels $\psi + K^{*0}$ and $\psi + K^\pm$ from CDF[24].

3.2 $B^0 - \overline{B}^0$ MIXING

The phenomenon of flavor oscillation, which produces mixing, has been first observed in the K^0- $\overline{K}^0$ system. It arises from $\Delta S = 2$ transitions (box diagrams) that change the K^0 into a $\overline{K}^0$. These transitions are allowed because the weak interactions do not conserve flavor. The effect is observable because the mass eigenstates, K_S and K_L, have a non zero mass difference, ΔM, and the K^0 lifetime is long enough for a number of oscillations (period $2\pi/\Delta M$) to occur before the K^0 system decays.

Mixing is therefore characterized by the parameter

$$x = \Delta M/\Gamma$$

Since the B lifetime is quite large, $B^0 - \overline{B}^0$mixing is observable for even small values of ΔM. The parameter x is related to some of the Cabibbo-Kobayashi-Maskawa matrix elements and to the top mass. The UA1 experiment[28] reported first the observation of mixing, later confirmed by the ARGUS and CLEO experiments[29].

Mixing has been measured in events where both the b and the $\bar{b}$ decay semileptonically, and the charge of the leptons tags the flavor of the b quark. A like-sign lepton pair indicates that one of the mesons has changed into its antiparticle. The magnitude of mixing is then measured

by determining the ratio, R, of like-sign (LS) to opposite-sign (OP) leptons. LS leptons can also be the result of a sequential b decay (i.e., $b \to c \to \ell$), therefore this has to be taken into account.

The mixing parameter χ gives the probability of a B^0 hadron to transform into its antiparticle. It is defined as:

$$\chi = \frac{(b \to \overline{B}^0 \to B^0 \to \ell^+ X)}{(b \to \ell^\pm X)} \qquad (2)$$

where the denominator includes all possible hadrons formed by the b quark. The relation between R and χ is:

$$R = \frac{N(LS)}{N(OS)} = \frac{2\chi(1-\chi) + [(1-\chi)^2 + \chi^2] f_s}{[(1-\chi)^2 + \chi^2] + 2\chi(1-\chi) f_s + f_c} \qquad (3)$$

with

$$f_s = N_s / N_f$$

$$f_c = N_c / N_f$$

where N_f is the number of first generation b decays, N_s the number of sequential decays, and N_c the number of events from $c\bar{c}$ decays.

At the $\Upsilon(4S)$ only B_d is produced, so CLEO and ARGUS measure χ_d, whereas at hadron colliders and LEP a combination of B_d and B_s is produced and therefore the quantity measured is:

$$\chi = P_d \chi_d + P_s \chi_s \qquad (4)$$

where

$$P_q = Prob(b \to \overline{B}_q^0) \frac{BR(\overline{B}_q^0 \to \ell^-)}{BR(b \to \overline{B} \to \ell^-)} \qquad (5)$$

We will discuss here the recent results of the CDF[30,24] and the UA1[31] collaborations.

CDF uses both the ee and the $e\mu$ channels for this analysis. Using $e\mu$ events has the advantage that the rate is high (twice that for ee or $\mu\mu$) and that there is no background from other lepton pair production mechanisms: Drell-Yan (DY), J/ψ, and Υ. For the $e\mu$ events the trigger used required an EM shower with $E_T > 5$ GeV and a muon with $P_T > 3$ GeV/c. For the ee sample the trigger required two electron clusters with $E_T > 5$ GeV.

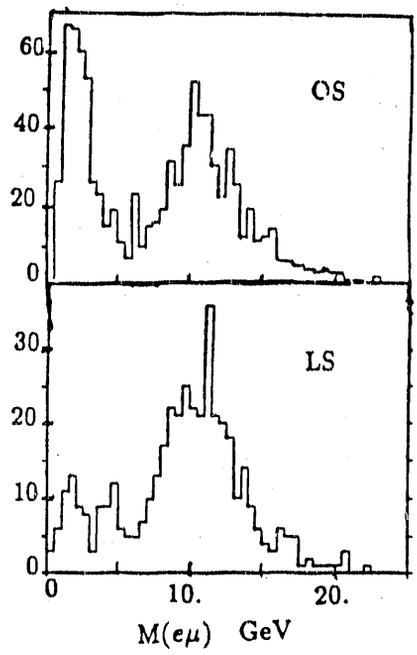

Figure 15: The invariant mass of the $e\mu$ system for like-sign (LS) and opposite sign (OP) pairs used by CDF for the study of mixing[24,30].

After applying the standard e and μ selection criteria[16,23], the opposite sign lepton events coming from same side sequential b decays (i.e. $b \to \ell^- c\ X, c \to \ell^+$) are removed by rejecting events for which the $\ell\ell$ invariant mass is $M(\ell\ell) < 5$ GeV. This distribution is shown in Figure 15 for the $e\mu$ events. For the ee events this removes the background from the J/ψ region, whereas the Υ region is explicitly removed by another mass cut. The number of events for the two channels are: 900 for the $e\mu$ (346 LS and 554 OS), 241 for the ee (92 LS and 149 OS).

For the $e\mu$ sample the major background comes from hadrons misidentified as leptons. This source contributes equally to the LS and OS samples. This has been studied using a sample of minimum-bias events, checked with data obtained with other e triggers and augmented by information extracted from the CDF Monte Carlo. It was found that the background fraction is (20 ± 10)%. After background removal the value of R is

$R = 0.552 \pm 0.049(\text{stat.})\ ^{+0.039}_{-0.048}(\text{syst.})$

For the ee events the backgrounds come from DY, photon conversions, Dalitz decays and from misidentified hadrons. Detailed studies of these background sources remove 45 ± 15 OS events and 11 ± 4 LS events from the sample. The

result for R is

$$R = 0.587 \pm 0.113(\text{stat}) \pm 0.043\ (\text{sys})$$

In the absence of mixing the expected values of R would be 0.23 ± 0.06 for the $e\mu$ channel and 0.24 ± 0.07 for the ee channel.

In order to extract χ from the R measurements using Eq. 3, it is necessary to calculate f_s and f_c for the two samples. This is done by using the ISAJET[21] Monte Carlo and the CDF detector simulation. The ratio of second to first generation semileptonic decays is found to be f_s=0.25 ± 0.06 for both channels. The error includes systematic uncertainties from b fragmentation, semileptonic branching ratios, and $b\bar{b}$ correlations coming from higher order processes. The ratio of charm to first generation b semileptonic decays, f_c, is found to be 0.07 ± 0.07 for the $e\mu$ events and 0.02 ± 0.02 for the ee channel.

These results lead to a combined value for χ of

$$\chi = 0.177 \pm 0.032(\text{stat+sys}) \pm 0.032\ (\text{Monte Carlo})$$

Figure 16 shows the observed μ spectra for the LS and OS $e\mu$ events compared with the Monte Carlo predictions.

The UA1 collaboration[31] uses di-muon events obtained in 4.7 pb^{-1} of data collected in the 1988-89 run. Muons are required to have $P_T > 3$ GeV/c and to be within the $|\eta| < 2.5$ region. The muons are also required to be non-isolated and have associated jet activities, with the jet axis being within a cone of Δ R = 1.0 with the muon. Again the variable P_T^{rel} is used. There are 889 events left after all cuts, of which 537 are LS and 352 are OS.

The ISAJET[21] Monte Carlo and the UA1 detector simulation are used to determine the shape of the P_T^{rel} distributions for the background, charm and sequential decays. These distributions are then used to fit the data with a maximum likelihood method. Absolute normalization for the background comes from the data. The DY and Υ background are obtained from data and Monte Carlo. The background is found to be (37.0 ± 9.2)% of the data, the $c\bar{c}$ contribution is (11.0 ± 5.5)% of the OS events and the DY is (1.2 ± 0.2)% of the OS events. Figure 17 shows the fits to the P_T^{rel} distributions for the lower and higher P_T

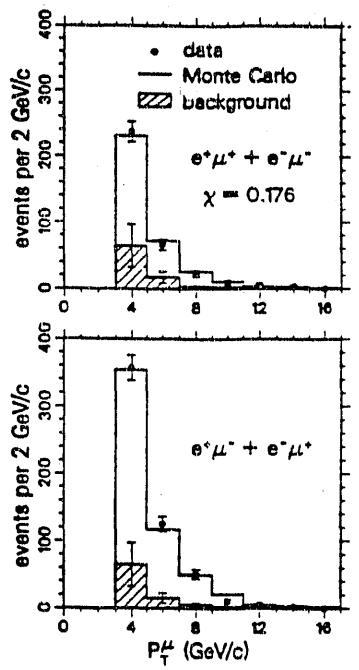

Figure 16: The muon P_T spectra for the like-sign and opposite sign $e\mu$ pair samples used by CDF to study mixing[24,30]. The data are shown as points, the Monte Carlo as histograms. The background is also shown.

muons. The final result of the analysis averaged with the previous UA1 result[28], gives:

$$\chi = 0.148 \pm 0.029(stat) \pm 0.017(sys) \quad UA1.$$

Recent measurements from LEP experiments[32] give:

$$\chi = 0.132^{+0.027}_{-0.026} \qquad ALEPH$$
$$\chi = 0.178^{+0.049}_{-0.040} \qquad L3$$

The next challenge is to obtain x_s which is related to χ_s by the relation:

$$x = \sqrt{2\chi/(1-2\chi)}$$

The average of the CLEO and ARGUS results[29] gives x_d = 0.72 ± 0.13. The Standard Model gives the relation[33]

$$\frac{x_s}{x_d} = \left[\frac{f_{B_s}}{f_{B_d}}\right]^2 \left[\frac{V_{ts}}{V_{td}}\right]^2 \tag{6}$$

where the f_i are form factors and V_i are CKM matrix elements. A limit on this ratio[33] from present fits of the

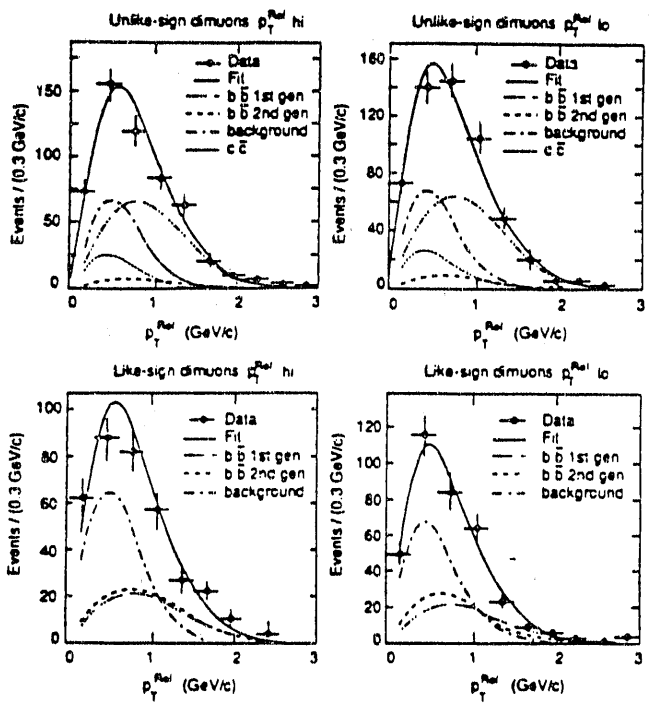

Figure 17: Distributions of muon P_T^{rel} from the UA1 di-muon events[31] The unlike and like sign and the higher and lower P_T muons are plotted separately. The data are plotted as points, the Monte Carlo as continuous lines.

CKM matrix parameters using existing data is:

$$\frac{x_s}{x_d} > 6.9 \qquad (7)$$

this implies that x_s is quite large.

In order to measure χ_s we need to know P_s and P_d in Eq. 3. Assuming P_d=0.375 and P_s = 0.150, it is possible to draw the curve in Figure 18, which shows the average of the ARGUS and CLEO results and the CDF result. This shows that from the Standard Model (Eqs. 6,7) and the CLEO-ARGUS results, the allowed region is very small and that χ_s is expected to be close to the maximum value of 0.5, i.e., that mixing in the B_s system is very large. The present measurements of χ_s, however, have very large uncertainties and are very far from testing the Standard Model. Clearly, measurements of P_d and P_s and much larger statistics or different methods will be needed. For example, the study of oscillations in the time dependence of B_s decays would provide a direct measurement of x_s.

3.3 RARE B DECAYS

Both UA1 and CDF have implemented di-muon triggers

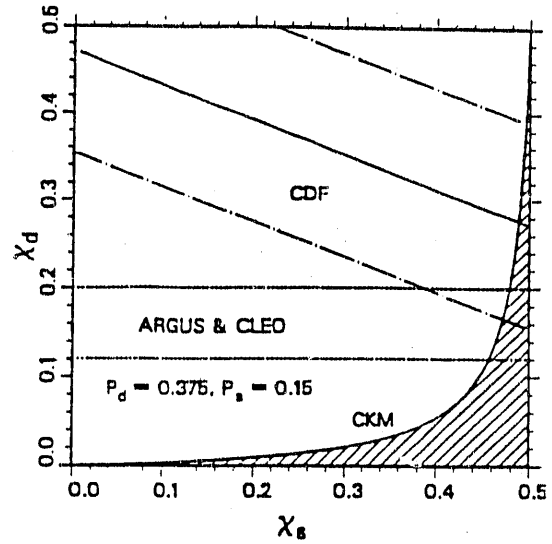

Figure 18: The mixing probability for B_d versus that for B_s. The u:d:s B production is assumed to be 0.375:0.375:0.150. The average of the ARGUS and CLEO results[29] as well as the CDF results[30] are shown. The shaded region is the prediction of the Standard Model.

that provide good statistics on J/ψ as well as on higher mass di-muons. This allows the study of rare decay modes like:

$$B \rightarrow \mu\mu \quad \text{and} \quad B \rightarrow \mu\mu + X$$

These transitions occur via flavor changing neutral currents (FCNC), which are allowed at the one loop level through the penguin diagrams. For $B \rightarrow \mu\mu$ the box diagram also contributes, and the branching ratio is expected to be of the order of 10^{-9}-10^{-8} (for a top mass in the 100-200 GeV range)[34].

CDF measured[24] the $B \rightarrow \mu\mu$ branching ratio by comparing its rate to the rate for $\psi' \rightarrow \mu\mu$. The sample used has been discussed in Sec. 3.1.2 and the data has been shown in Figure 13. The $\mu\mu$ invariant mass for the ψ' and the B regions are shown in Figure 19. The fitted curves give $N_{\psi'} = 72 \pm 17$ events and $N(B \rightarrow \mu\mu) = 0.28\ ^{+7.15}_{-6.47}$ events above background. This corresponds to N< 12 (at 90% C.L.).

To obtain an absolute branching ratio the assumption is made that all the ψ' come from B decays. This assumption is based on the model by Glover et al[35] which predicts that direct $p\bar{p} \rightarrow \psi' + X$ production is very small. The ratio of

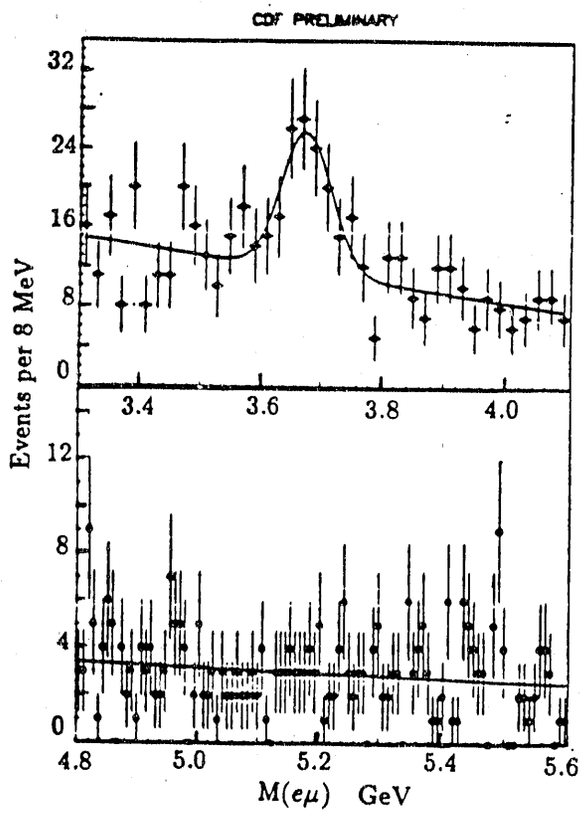

Figure 19: The $\mu\mu$ invariant mass measured by CDF[24] in two different mass intervals: the ψ' region (top) and the B region (bottom).

acceptances for the two channels is found to be about 4. The ψ' branching ratio, averaged from the CLEO[36] and ARGUS[26] results, and using the PDG value for $\psi' \to \mu\mu$, is

$$BR(B \to \psi') \times BR(\psi' \to \mu\mu) = (2.8 \pm 1.2)10^{-5}$$

This gives

$$BR(B \to \mu\mu) < 3.2 \times 10^{-6} \quad (90\%C.L.) \quad CDF$$

The UA1 analysis[37] is done on an integrated luminosity of 5.3 pb^{-1}, including the data discussed in Sec 3.1.1 and data taken in earlier runs. The $\mu\mu$ invariant mass for the region of interest is shown in Figure 20. Muon pairs with $P_T > 6$ GeV/c are used. In the B region they observe 6 events on a background of 5.0 ± 1.0 events. Using an efficiency in their acceptance region of (4.0 ± 1.7)% as calculated using the ISAJET Monte Carlo and the b cross section measured by UA1 (see Sec. 3.1.1), they obtain

$$BR(B \to \mu\mu) < 8.3 \times 10^{-6} \quad (90\%C.L.) \quad UA1$$

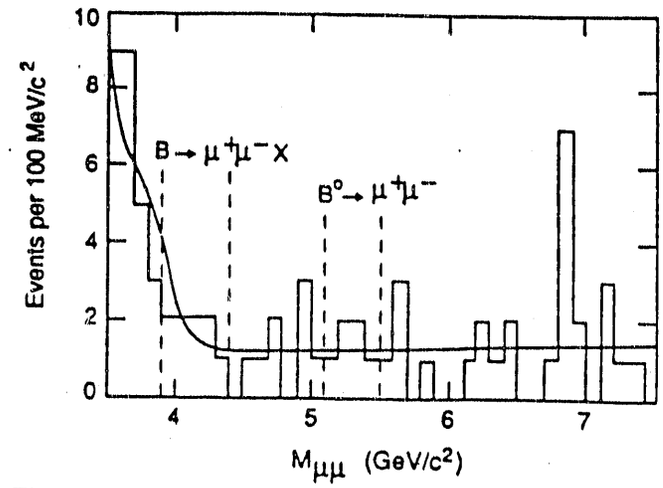

Figure 20: The $\mu\mu$ invariant mass measured by UA1[37] in the high mass region. Regions used for the B→ $\mu\mu$ and B→ $\mu\mu X_s$ decay modes are indicated by dashed lines.

For the B→ $\mu\mu + X_s$ search a M($\mu\mu$) mass region between 3.9 and 4.4 GeV is chosen, in order to avoid regions of interference between the matrix elements of the B→ ψ' decay mode and the penguin diagrams, as discussed in the UA1 paper[37]. This cut reduces the acceptance to (1.1 ± 0.3)%. UA1 observes 9 events on a background of 8.7 ± 1.7 and obtains:

$$BR(B \to \mu\mu X_s) < 5.0 \times 10^{-5} \quad (90\%C.L.) \quad UA1$$

With the same data UA1 also searched for $B \to \mu\mu K^{*0}$, by looking for a K^{*0} signal in the associated tracks in a cone of ΔR =1.0 around the direction of the $\mu\mu$ system. The requirements on the two muons are less stringent to increase efficiency, the K^* tracks are required to be above 100 MeV/c and the K^* to have a $P_T > 2$ GeV/c. They observe two events in the data with a background of 1.0 ± 0.6 events. With an efficiency of (1.1 ± 0.3)% they obtain:

$$BR(B^0 \to \mu\mu K^{*0}) < 2.3 \times 10^{-5} \quad (90\%C.L.) \quad UA1$$

The limits obtained by both CDF and UA1 are lower than the published results from ARGUS[26] and CLEO[38] of 5×10^{-5} for $B^0 \to \mu\mu$, 2.4×10^{-3} for $B^0 \to \mu\mu + X_s$ and 1.9×10^{-4} for $B^0 \to \mu\mu K^{*0}$.

4.0 SUMMARY AND FUTURE PROSPECTS

The search for the top quark will be the domain of hadron colliders over the next few years. Present limits

are:

$m_t > 89$ GeV from CDF, standard decay modes[1]

$m_t < 210$ GeV from fits to the Standard Model[2].

For the Tevatron Collider run in 1992, CDF will have improved acceptance for the muon system and improved b tagging capability using the silicon vertex detector (SVX), which is being installed. The integrated luminosity for the run is expected to increase the present CDF statistics by a factor five. A new detector, D0, will be taking data, thus increasing the overall chance of detecting the top. A mass reach of 130 GeV should be possible.

The b physics potential of hadron colliders is becoming evident. The predicted cross sections are very large[3,4] and measurements done by UA1[20,22] and CDF[24] seem to confirm the QCD predictions. Mixing has been observed at hadron colliders first; the new results by both UA1 and CDF have been summarized here. Limits on rare decay modes reported by UA1 and CDF have improved existing limits from e^+e^- machines by one order of magnitude in some cases. Prospects for studies of exclusive channels look very good.

B physics capabilities for the next collider run should improve by large factors. CDF expects to gain by an order of magnitude[19] in efficiency and has added capabilities in b tagging due to the installation of the SVX. D0 has an excellent muon detector which can be exploited for b tagging. Measurements of lifetimes for different b charges and species should be possible, as well as studies of exclusive decay modes. The next collider run should also provide enough data to allow understanding on whether CP violation can be studied in hadron colliders.

7 REFERENCES

1. K. Sliwa (CDF Collab.), "A New limit on the mass of the top quark", Proceedings of the XXVth Rencontres de Moriond, Les Arcs, Savoie, France (March 1990). See also G.P.Yeh, Proceedings of Les Rencontres de Physique de La Vallee D'Aoste, La Thuile, Italy, p. 451 (March 1990).
2. V. Barger et al., Phys. Rev. Lett. 65, 1313 (1990); J. Ellis and G. Fogli, Phys. Lett. B249, 543 (1990), $m_t < 202$ GeV; P. Langacker and M. Luo, University of Pennsylvania preprint UPR-0466T (Feb. 1991), $m_t < 182$ GeV; P. Langacker, Phys. Rev. Lett. 63, 1920 (1989), and references therein.
3. R. K. Ellis, Proceedings of the SLAC Summer Institute on Particle Physics, p. 45 (1989).
4. P. Nason, S. Dawson and R.K. Ellis, Nucl. Phys. B303, 607 (1988); and Nucl. Phys. B327, 49 (1989).
5. M. Diemoz, F. Ferroni, E. Longo and G. Martinelli, Z. Phys. C39, 21 (1988).
6. G. Altarelli, M. Diemoz, G. Martinelli and P. Nason, Nucl. Phys. B308, 724 (1988).
7. C. Albajar et al. (UA1 Collab.), Z. Phys. C48, 1 (1990).
8. T. Acheson et al.(UA2 Collab.), Z. Phys. C46, 179 (1990).
9. F. Abe et al., (CDF Collab.), Phys. Rev. Lett. 64, 142 (1989).
10. F. Abe et al., (CDF Collab.), Phys. Rev. Lett. 64, 147 (1989).
11. J. F. Gunion, H.E. Haber, G. Kane, S. Dawson, "The Higgs Hunter Guide", Addison Wesley (1990).
12. C. Albajar et al., (UA1 Collab.), Phys. Lett. B257, 459 (1991).
13. F. Dydak, Review of LEP Results, Proceedings of the 25th International Conference on High Energy Physics, Singapore, p. 3 (August 1990).
14. Abe et al., (CDF Collab.), Phys. Rev.D44, 29 (1991).
15. J. Alitti et al. (UA2 Collab.) CERN preprint PPE-91-162 (1991); and (previous result) J. Alitti et al., Phys. Lett. B241, 150 (1990).
16. F. Abe et al., (CDF Collab.), Phys. Rev. Lett. 65, 2243 (1991), and Phys. Rev.D43, 2070 (1991).
17. F. Halzen,B. A. Kniehl, Nucl. Phys. B353, 567 (1991).
18. S. Lloyd, 1991 Aspen Winter Conference in Elementary Particles, (January 1991).
19. H. Wenzel, these Proceedings
20. C. Albajar et al., (UA1 Collab.), Phys. Lett. B256, 121 (1991).
21. F. Paige and S. D. Protopopescu, Brookhaven report BNL-38034 (1986).
22. C. Albajar et al., (UA1 Collab.), Phys. Lett. B256, 112 (1991).

23. F. Abe et al. (CDF Collab.), Phys. Rev. 43, 664 (1991).

24. A. Sansoni (CDF Collab.), Proceedings of the XXVI Rencontre de Moriond, (March 1991). P. Sinervo, Proceedings of Les Rencontres de Physique de La Vallee D'Aoste, LaThuile, Italy (March 1991).

25. C. Bebek et al., (CLEO Collab.) Phys. Rev. D36, 1289 (1987).

26. H. Albrecht et al., (ARGUS Collab.) Phys. Lett. B199, 451 (1987).

27. C. Peterson et al., Phys. Rev. D27, 105 (1983).

28. C. Albajar et al. (UA1 Collab.), Phys. Lett. B186, 247 (1987).

29. H. Albrecht et al., (ARGUS Collab.), Phys. Lett. B192, 245, (1987). M. Artuso et al., (CLEO, Collab.), Phys. Rev. Lett. 62, 2233 (1989).

30. F.Abe et al., (CDF collab.), "Measurement of the $B^0 - \overline{B}^0$Mixing at the Fermilab Tevatron Collider", to be published in Phys. Rev. Lett. (1991).

31. C.Albajar et al., (UA1 Collab.), Phys. Lett. B262, 171 (1991).

32. B. Adeva (L3 Collab.), Phys. Lett. B252, 703 (1991); D. Decamp et al., (ALEPH Collab.), Phys. Lett. B258, 236 (1991).

33. C.S. Kim, J.L. Rosner, C.P. Yuan Phys. Rev. D42, 96 (1990). For the formalism see also P.J. Franzini, Phys. Rep. 173, 1 (1989).

34. J.L.Hewett et al., Phys. Rev. D39, 250 (1989).

35. E.W.N. Clover et al., Z. Phys. 38C, 473 (1988).

36. W.Y. Chen (CLEO Collab.), Thesis, Purdue University, PU-90-646 (1990).

37. C. Albajar et al., Phys. Lett. B262, 163 (1991).

38. A. Bean et al., (CLEO Collab.) Phys. Rev. D35, 3533 (1987); P. Avery et al., (CLEO Collab.) Phys. Lett. B223, 470 (1989).

END

DATE FILMED

7/13/92